ISSN 1392–1320 MATERIALS SCIENCE (MEDŽIAGOTYRA). Vol. 11, No. 3. 2005

Influence of Strain Rate and Temperature on Mechanical Properties and Fracture Mechanism of Dispersion Strengthened Al-12Al_4C_3 System

Olga VELGOSOVÁ[1*], Michael BESTERCI[2], Priit KULU[3]

[1]*Technical University Faculty of Metallurgy, Department of Non-ferrous Materials and Waste Treatment, Letná 9/A, Košice 04200, Slovakia*
[2]*Institute of Materials Research, Slovak Academy of Sciences, Watsonova 47, Košice 043 53, Slovakia*
[3]*Tallin University of Technology, Etritajate tee 5, 19086 Tallinn, Estonia*

Received 27 May 2005; accepted 08 July 2005

In the presented work the change in fracture for the Al-12Al_4C_3 system was investigated and analysed at temperatures from 20 to 400 °C and strain rates from $2.5\cdot10^{-5}$ to 10^{-1} s^{-1}. At room temperature 20 °C, during tensile testing at strain rates in the tested region, the strain is first controlled by work hardening, expressed by the exponent *n*. In the second generally smaller part the deformation is limited by local straining and forming the neck. There is a marked decrease of plastic properties for the strain rate $\dot{\varepsilon} = 2.5\cdot10^{-5}$ s^{-1} with the growth of temperature in the investigated region. It is explained by changes in the micromechanism of deformation and fracture. Fracture surface shows the transition from ductile fracture with dimples at 20 °C, to intercrystalline fractures, with the growth of the temperature, an indication of exhausted grain boundary plasticity. The intercrystalline fracture initiation tends, it is supposed, to be localized in triple points. At temperatures 400 °C, and $\dot{\varepsilon} = 10^{-1}$ s^{-1} there is a marked growth of plastic properties. The first part of the strain characterized by work hardening is very short. After the short growth of the stress to maximum, a deformation mechanism, showing presence of thermally and mechanically activated dynamic recovery processes takes place. The strain is this way uniform all over the body of the test piece. The fracture process ends with the increase of cavities and transcrystalline fracture with deep pimples.

Keywords: dispersion strengthened materials, mechanical properties, fracture mechanism, TEM and SEM analysis.

1. INTRODUCTION

The dispersion strengthened alloys Al-Al_4C_3 prepared by mechanical alloying using powder metallurgy technology are promising structural materials enabling significant cuts of weight for use first in aircraft and car industry, also at elevated temperatures [1 – 3]. We have described in work [4] the optimised production technology by mechanical alloying.

In work [5] the mechanical properties and plasticity at elevated temperatures were analysed. In [6] the high temperature stability of this alloy is described for long time exposition. In [7] the changes in microstructure were observed and analyzed after deformation at elevated temperatures, and in [8] the mechanism of fracture in creep were studied.

In [9, 10] was described the model of "in-situ" fracture mechanism of these materials. Kinetics and mechanism of superplastic deformation of Al alloys are analyzed in works [11 – 16].

In the present work we analyze the fracture at different strain rates and temperature. Temperatures from 20 to 400 °C and strain rates from $2.5\cdot10^{-5}$ to 10^{-1} s^{-1} had been used. Considering the results reported in [17] and the strain induced coefficient m ranging from 0.03 to 0.06 we have covered the strain rates from creep to the activation of superplastic behavior.

2. EXPERIMENTAL. MATERIAL AND METHODS

The Al-Al_4C_3 composite dispersion strengthened by 12 vol.% of Al_4C_3, has been prepared by the method of mechanical alloying. The milling of the Al powder grain size under 100 μm with 1 % of KS 2.5 graphite lasted 90 minutes. Granulate was compacted under the pressure of 600 MPa and annealed at 550°C with a 94 % reduction.

Fig. 1. Microstructure of Al-12Al_4C_3 material

The dispersed particles are oriented in layers in the direction of extrusion, Fig. 1. The effective size of the particles as measured on the foils was 25×85 nm. There

* Corresponding author. Tel.: +421-55-6336401; fax.: +421-55-7922408.
E-mail address: *oksana.velgosova@tuke.sk* (O. Velgosova)

were larger dispersed particles, too. They ranged from 85 nm to 1 μm in size, making up about 30 % of dispersed amount, observed by Scanning Electron Microscopy (SEM) and metallography. The Al_4C_3 and Al_2O_3 particles are on grain boundaries as well as inside in Al grains. The observed microstructure is fine, even, with grains less than 1 μm, elongated in the direction of extrusion, Fig. 2.

Fig. 2. The foil of Al-12Al_4C_3 material

Test pieces 3 mm in diameter and 15 mm gauge length had been machined for tensile test. They were positioned in longitudinal direction, in respect to the direction of extrusion. For the evaluation of strain and fracture mechanisms SEM examined fracture surfaces.

3. RESULTS AND DISCUSSION

The results are summarised in Fig. 3, where the yield strength $R_p0.2$ and the reduction of area Z are plotted in dependence on the test temperature and strain rate applied. Note that by temperature 400 °C and strain rate 10^{-1} s^{-1} occur rapid increase in value Z but the value of yield strength don't remark the substantial changes. Corresponding results were obtained for UTS and elongation.

For high strain rate $\dot{\varepsilon} = 10^{-1}$ s^{-1} and temperature 20 °C the fracture surface is presented in Fig. 4. For low strain rates $\dot{\varepsilon} = 2.5 \cdot 10^{-5}$ s^{-1} it is in Fig. 5. There are no significant differences between them. Both are ductile, transcrystalline fractures with dimples. The dimples are shallow with a characteristic dimension 0.45 μm.

Fracture surfaces fractured at strain rate $\dot{\varepsilon} = 2.5 \cdot 10^{-5}$ s^{-1} and temperature 300 °C showed underdeveloped intercrystalline facets. They are underdeveloped because at the end of fracture, a ductile fracture takes place. At the strain rate $\dot{\varepsilon} = 10^{-1}$ s^{-1} the fracture is transcrystalline with dimples. The dimples are deeper and larger then those at 20 °C. The characteristic dimple diameter is around 0.6 μm.

At low strain rate $\dot{\varepsilon} = 2.5 \cdot 10^{-5}$ s^{-1} and temperature 400 °C the fracture took place at $Z = 8$ %. Typical micro facets of the fracture are shown in Fig. 6. Prevailingly, developed intercrystalline facets are present, with dimensions corresponding to the fine grain size, and great angle disorientation. There are small parts of fracture showing crests of ductile facets. For the strain rate $\dot{\varepsilon} = 10^{-1}$ s^{-1} the fracturing ended at a reduction of area $Z = 64$ %. The fracture is ductile transcrystalline with developed deep dimples Fig. 7. The characteristic dimple dimension is 0.65 μm.

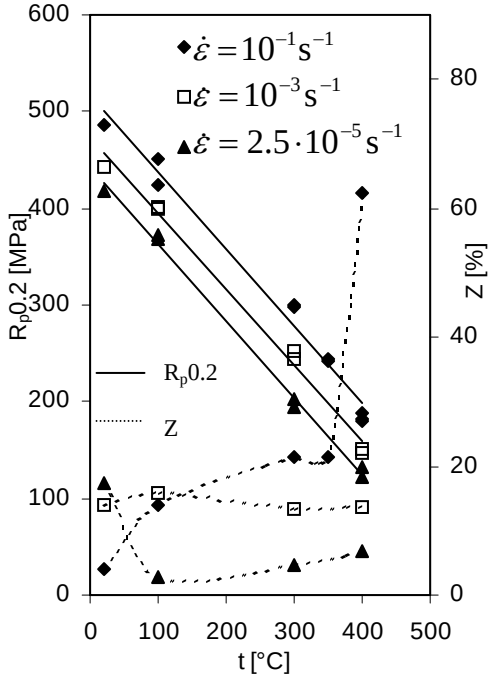

Fig. 3. Influence of temperature and strain rate on yield strength $R_p0.2$ and reduction of area Z

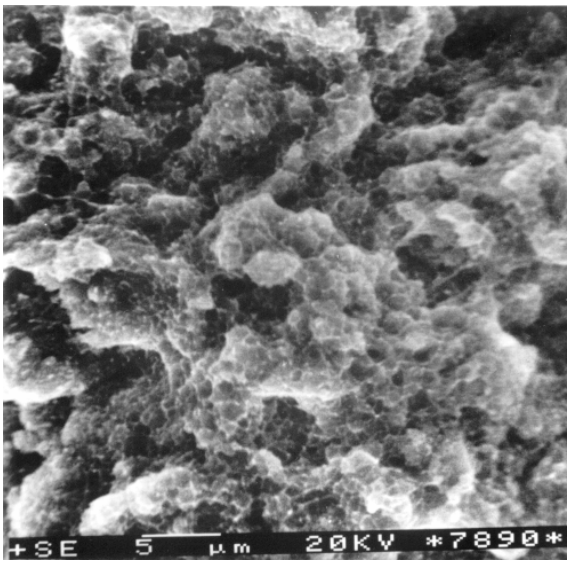

Fig. 4. Transcrystalline fracture surface obtained with strain rate 10^{-1} s^{-1} and temperature 20 °C

The dependence the middle dimples diameter of temperature for strain rate 10^{-1} s^{-1} is seen on Fig. 8. The analysis of fracture at 400 °C and strain rate $\dot{\varepsilon} = 2.5 \cdot 10^{-5}$ s^{-1} has shown intercrystalline fractures, as the result of damage to grain boundaries formed by interactions of dislocations with dispersed particles on grain boundaries. However, the fine particles on grain boundaries are

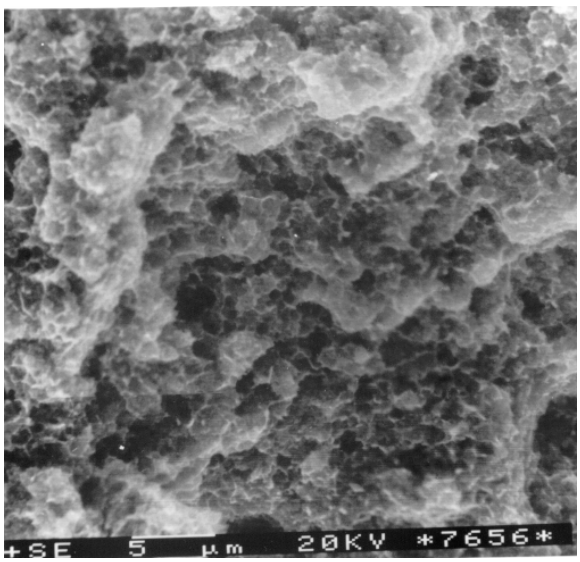

Fig. 5. Transcrystalline fracture surface obtained with strain rate $2.5 \cdot 10^{-5}$ s^{-1} and temperature 20 °C

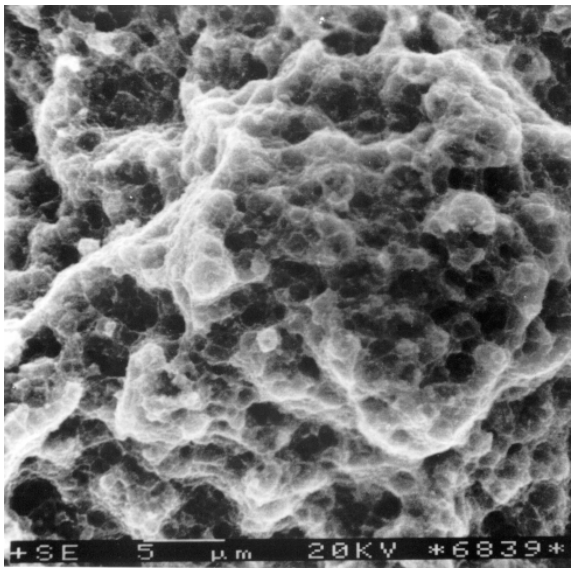

Fig. 6. Intercrystalline fracture surface obtained with strain rate $2.5 \cdot 10^{-5}$ s^{-1} and temperature 400 °C

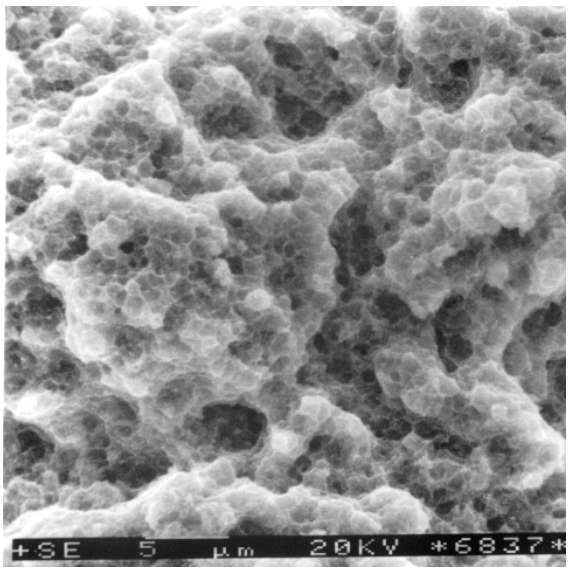

Fig. 7. Transcrystalline fracture surface obtained with strain rate 10^{-1} s^{-1} and temperature 400 °C

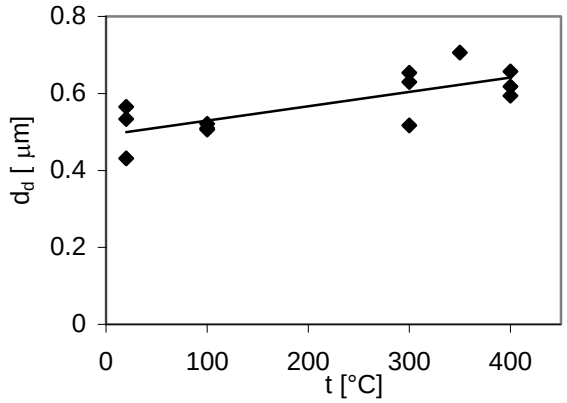

Fig. 8. The dependence of the middle dimple diameter on temperature for strain rate 10^{-1} s^{-1}

important for diffusion creep and strength properties at high temperatures. Transcrystalline fractures at high strain rates (10^{-1} s^{-1}) show a remarkable recovery in the plato part of the stress-strain curve, a dynamic polygonisation resulting in a dynamic equilibrium of strengthening and weakening. The fracture is caused by voids occurring on the interfaces dispersed-matrix first on larger particles, after a great amount of strain. The voids are growing and coalescence into dimples of the transcrystalline fracture.

4. CONCLUSIONS

At room temperature 20 °C, during tensile testing at strain rates in the tested region, the strain is first controlled by work hardening, expressed by the exponent *n*. In the second generally smaller part the deformation is limited by local straining and forming the neck.

There is a marked decrease of plastic properties for the strain rate $\dot{\varepsilon} = 2.5 \cdot 10^{-5}$ s^{-1} with the growth of temperature in the investigated region. It is explained by changes in the micromechanism of deformation and fracture. Fracture surface shows the transition from ductile fracture with dimples at 20 °C, to intercrystalline fractures, with the growth of the temperature, an indication of exhausted grain boundary plasticity. The intercrystalline fracture initiation tends, it is supposed, to be localized in triple points.

At temperatures 400 °C, and $\dot{\varepsilon} = 10^{-1}$ s^{-1} there is a marked growth of plastic properties. The first part of the strain characterized by work hardening is very short. After the short growth of the stress to maximum, a deformation mechanism, showing presence of thermally and mechanically activated dynamic recovery processes takes place. The strain is this way uniform all over the body of the test piece. The fracture process ends with the increase of cavities and transcrystalline fracture with deep dimples.

Acknowledgments

This work has been supported by grant 2/2114/22.

REFERENCES

1. **Jangg, G., Kutner, F., Korb. G.** Dispersionsgehärteten Al-Al_4C_3 Werkstoffen *Aluminium* 51 1975: pp. 641 – 645.

2. **Jangg, G., Korb G., Kutner**, **F.** Dispersionenvestigten Werkstofen auf bases Al *In: 6. Internationale Leichtmetall-ltagung, Aluminiuum Verlag*, Dusseldorf 1977: pp. 23 – 25.
3. **Korb, G., Jangg, G., Kutner, F.** Mechanism der dispersionenvestigten Al-Al_4C_3 Werkstoffen *Draht* 5 (1) 1979: pp. 318 – 324.
4. **Šlesár, M., Jangg, G., Besterci, M., Ďurišin**, **J.** Structur und mechanik die Eingeschaften von dispersiongehärteten Al-Al_4C_3 Werkstofen *In: Internationale Leichtmetalltagung*, Leoben-Wien, 1981: pp. 238 – 240.
5. **Šlesár, M., Besterci M., Jangg, G., Miškovičová, M., Pelikan K.** Einfluss der Temperatur und Festigkeit und Plasticität von dispersionsverfestigten Al-Al_4C_3 Werkstofen *Z. Metallkunde* Bd.79 (H1) 1988: pp. 56 – 62.
6. **Šlesár, M., Jangg, G., Besterci M., Ďurišin**, **J., Orolínová M.** Temperaturstabilität des Subgefuges von dispersiongehärteten Aluminium *Z. Metalkunde* Bd. 80 (H11) 1989: pp. 817 – 824.
7. **Šlesár, M., Jangg, G., Ďurišin**, **J., Besterci M., Orolínová M.** Änderungen des Gefüges von Al-Al_4C_3-Werkstoffen durch Verformungsverfestigung und thermische Entfestigung *Mat-Wiss. U. Werkstoffmechanik* 23 (1) 1992: pp. 13 – 17.
8. **Šlesár, M., Besterci M., Jangg, G.** Bruch charakteristic des dispersionsverfestigten Al-Al_4C_3 Werkstofen beim Kriechen *Z. Metallkunde* Bd. 83 (H3) 1992: pp. 183 – 189.
9. **Besterci M., Ivan, I.** Failure Mechanism of Dispersion Strengthened Al-Al_4C_3 Systems *J. of Mat. Sci. Letters* 15 23 1996: pp. 2071 – 2074.
10. **Besterci M., Ivan, I., Velgosová, O., Pešek**, **L.** Damage Mechanism of Al-Al_4C_3 System with High Volume Fraction of Secondary Phase (Mechanizmus porušovania sústavy Al-Al_4C_3 s vysokým objemovým podielom sekundárnej fázy) *Kovové Mater.* 39 (6) 2001: pp. 361 – 367 (in Slovak).
11. **Mishra R.S., Mukherjee**, **A. K.** The Rate Controlling Deformation Mechanism in High Strain Rate Superplasticity *Metar. Sci. Eng.* A234 – A236 1997: pp. 1023 – 1025
12. **Mishra, R.S., Bieler, T.R., Mukherjee**, **K.** Superplastic Behaviour of Mechanically Alloyed Aluminium *Scripta Metall.* 26 1605 1992: pp. 1605 – 1608.
13. **Bieler T.R., Mukherjee**, **A.K.** Superplastic Deformation Mechanism(s) of Mechanically Alloyed Aluminum *Mater. Trans. JIM* 32 1991: pp. 1149 – 1158.
14. **Nieh, T.G., Wadsworth, J., Imai**, **T.** Arheological View of High-strain-rate Superplasticity in Alloys and Metal-matrix Composites *Scripta Metall. Mater.* 26 (5) 1992: pp. 703 – 708.
15. **Sakai M., Muto**, **H.** A Novel Deformation Process in an Aggregate: a Candidate for Superplastic Deformation *Scripta Mater.* 38 (6) 1998: pp. 909 – 915.
16. **Urena, A., de Salazar, J.M.G., Qiunones, J., Martin, J.J.** TEM Characterization of Diffusion Bonding of Superplastic 8090 Al-Li alloy *Scripta Mater.* 34 (4) 1996: pp. 617 – 623.
17. **Bieler, T.R., Nieh, T.G., Wadsworth, J., Mukherjee, A.** Superplastic-like Behavior at High Strain Rates in Mechanically Alloyed Aluminum *Scripta Metallurgica et Materialia* 22 1988: pp. 81 – 86.